Intravoxel Incoherent Motion Quantification Dependent on Measurement SNR and Tissue Perfusion: A Simulation Study

Sam Sharifzadeh Javidi (PhD Candidate)[1,2], Alireza Shirazinodeh (PhD Candidate)[1], Hamidreza Saligheh Rad (PhD)[1,2]*

[1]Department of Medical Physics and Biomedical Engineering, Medicine School, Tehran University of Medical Sciences, Tehran, Iran
[2]Quantitative Medical Imaging Systems Group, Research Center for Molecular and Cellular Imaging, Tehran University of Medical Sciences, Tehran, Iran

ABSTRACT

Background: The intravoxel incoherent motion (IVIM) model extracts both functional and structural information of a tissue using motion-sensitizing gradients.

Objective: The Objective of the present work is to investigate the impact of signal to noise ratio (SNR) and physiologic conditions on the validity of IVIM parameters.

Material and Methods: This study is a simulation study, modeling IVIM at a voxel, and also done 10,000 times for every single simulation. Complex noises with various standard deviations were added to signal in-silico to investigate SNR effects on output validity. Besides, some blood perfusion situations for different tissues were considered based on their physiological range to explore the impacts of blood fraction at each voxel on the validity of the IVIM outputs. Coefficient variation (CV) and bias of the estimations were computed to assess the validity of the IVIM parameters.

Results: This study has shown that the validity of IVIM output parameters highly depends on measurement SNR and physiologic characteristics of the studied organ.

Conclusion: IVIM imaging could be useful if imaging parameters are correctly selected for each specific organ, considering hardware limitations.

Citation: Sharifzadeh Javidi S, Shirazinodeh AR, Saligheh Rad HR. Intravoxel Incoherent Motion Quantification Dependent on Measurement SNR and Tissue Perfusion: A Simulation Study. *J Biomed Phys Eng*. 2023;13(6):555-562. doi: 10.31661/jbpe.v0i0.2102-1281.

Keywords

Reproducibility of Results; Diffusion-Weighted Imaging; Perfusion Imaging; Intravoxel Incoherent Motion; SNR; Magnetic Resonance Imaging

Introduction

The diffusion of water molecules varies in different environments because it is based on the medium diffusion coefficient. Stejskal-Tanner developed a pulse sequence to map diffusion coefficient using diffusion decay of magnetic resonance imaging (MRI) signal [1]. Although diffusion-weighted imaging (DWI) was able to estimate the water diffusion coefficient in the non-living surrounding environment at each voxel, the first practical problem of this estimation in the living tissues was the unwanted motion of microcirculation in the capillary network. In 1986, Le Bihan et al. used DWI in-vivo for the first time [2]. In order to eliminate the blood-related diffusion signal decay, appeared in lower *b*-values, Le Bihan et al. suggested using multiple *b*-values (extended to the higher values) to reduce the effects of blood flow [3].

*Corresponding author: Hamidreza Saligheh Rad Quantitative Medical Imaging Systems Group, Research Center for Molecular and Cellular Imaging, Emam Khomeini Hospital, Keshavarz Boulevard, Tehran, Iran
E-mail: hamid.saligheh@gmail.com

Received: 12 February 2020
Accepted: 28 March 2021

Copyright: © Journal of Biomedical Physics and Engineering
This is an Open Access article distributed under the terms of the Creative Commons Attribution-NonCommercial 4.0 Unported License, (http://creativecommons.org/licenses/by-nc/4.0/) which permits unrestricted use, distribution, and reproduction in any medium, provided the original work is properly cited non-commercially.

Although blood flow was a kind of signal artifact in the first place, it was deployed as a source of perfusion information then [4]. Le Bihan et al. suggested a model where blood movement behavior was similar to diffusion random walk and named *pseudodiffusion* (D^*). This model - known as intravoxel incoherent motion (IVIM) - has three parameters: 1- true diffusion (D) of water molecules in a voxel, 2- the fraction of blood at each voxel (f) and 3- pseudodiffusion of a voxel (D^*).

IVIM imaging is very powerful because it not only provides the information of classic diffusion imaging accurately, but also extracts information about perfusion imaging. Several clinical and simulation studies have shown that IVIM imaging is a promising technique to diagnose abnormalities in brain, liver, kidney, breast, and prostate [5-10]. There is no need for exogenous contrast agent injection to extract IVIM perfusion information, which is the main limitation of classical perfusion MRI. Therefore, the IVIM imaging is really valuable when the patients cannot take exogenous contrast agents for classical perfusion MRI especially for patients with kidney malfunctioning.

Le Bihan et al. linked f and D^* with physiological parameters. When f is proportional to blood volume, D^* is linked to the inverse of mean transit time (MTT), and $f \times D^*$ is proportional to blood flow [11]. Some studies have investigated the relation between IVIM parameters and classical perfusion imaging. For example, Lee et al. reported moderate to good correlations between IVIM and dynamic contrast-enhanced MRI (DCE-MRI) in cervical cancer [12]. In addition, Federau et al. have shown that IVIM perfusion fraction f correlated well with dynamic susceptibility contrast - cerebral blood volume (DSC-CBV) [13]. Also, a correlation of arterial spin labeling (ASL) cerebral blood flow and $f \times D^*$ is reported [14, 15].

The first IVIM images were not successful because of low main field (0.5 T), low gradient strength (b-value less than 200 s/mm^2), and also slow imaging methods. Consequently, signal to noise ratio (SNR), sensitivity to diffusion, and also motion artifact corrupted image quality were low. Advances in technology such as higher main field (3T), stronger gradient (b-values more than 3000 s/mm^2), and fast imaging methods such as Ecko-planar imaging (EPI) paved the way in IVIM for the practical use [16]. For example, the use of a higher magnetic field (B0)- 3 T instead of 1.5 T- proved that there was significant robustness in f and D^* [17].

IVIM model is nonlinear, and the calculation of IVIM parameters are not straightforward. Several solutions have been suggested until now to improve the validity of output parameters [18-21]. Despite their pros and cons, all of them are affected by the low SNR of the imaging system. Furthermore, the selection of the optimum b-values is under question and reported differently for various organs [22-25]. In this paper, we investigated the impacts of SNR and blood fraction on the validity of IVIM results, which suggested a simple rule to ensure the validity of IVIM parameters.

Material and Methods

This is a simulation and analytical study in order to examine the impact of SNR and physiologic conditions on the accuracy and reproducibility of IVIM parameters. IVIM model is based on two-component DWI as follows: 1) One component is due to diffusion signal decay of water molecules as a result of thermal energy movement. 2) The second one describes perfusion signal decay resulted from blood circulation in the microvessel network. Then the IVIM model is formulated as:

$$\frac{S_b}{S_0} = (1-f)e^{-bD} + fe^{-bD^*} \qquad (1)$$

where S_b is the diffusion-weighted signal intensity of a b-value, S_0 is observed signal amplitude without diffusion gradient (b=0), f is blood fraction at each voxel, D is true diffusion coefficients, and D^* is pseudodiffusion

coefficients. Because of the nonlinear behavior of the IVIM model, there is no explicit (unique) solution. To the best of our knowledge, the most common method is based on a hypothesis that for higher *b*-values, the perfusion portion of signal decay is quite negligible (less than 1 percent or even less than noise floor). Therefore, D is calculated from a signal, derived by high *b*-values, in general, more than 250 *s/mm*^{2}.

$$\frac{S_{b_2}}{S_{b_1}} \propto \frac{(1-f)e^{-b_2 D}}{(1-f)e^{-b_1 D}} = e^{(b_1-b_2)D} \rightarrow D = \frac{\log \frac{S_{b_2}}{S_{b_1}}}{b_1 - b_2} \quad (2)$$

Perfusion parameters (f and D^*) can be computed using a known D.

Although all IVIM parameters are calculable, the validity of them in the presence of noise is in question. Therefore some questions are asked, as follows: 1) what is the least SNR to do IVIM imaging and how the validity of output is well-preserved? 2) when perfusion portion of signal decay is small enough that it is hard to observe; however, it is not observable because its amount approaches zero or less than noise floor. In other words, for which *b*-values is signal decay just based on diffusion and insensitive to perfusion movement signal decay? Some computer simulations were designed to investigate the impacts of SNR on the validity of parameters and also to see whether the least acceptable SNR varies in distinct organs or not. Validity was assessed by computing coefficient variation (CV) and bias of the estimator, where CV and bias are criteria for the precision and the accuracy of estimates.

$$CV = \frac{\sqrt{\frac{1}{N}\sum_{n=1}^{N}(x_i - x)^2}}{x} \quad (3)$$

$$Bias = \frac{\frac{1}{N}\sum_{n=1}^{N}(x_i - x)}{x} \quad (4)$$

I. Simulations

In the first experiment for a given voxel data such that D=0.001 mm^2/s, f=0.1 and D^*=0.01 mm^2/s, an in-silico signal was artificially generated based on the IVIM model with 10 *b*-values *b*=(0, 10, 20, 30, 50, 100, 200, 400, 600, 800 *s/mm*^{2}), and a complex Gaussian noise was added to it. The standard deviation of noise (σ_n) and S_0 define SNR parameters in our simulation such that:

$$SNR = \frac{Mean\ Signal}{Standard\ Deviation\ Noise} = \frac{S_0}{\sigma_n} \quad (5)$$

SNR amounts varied between [40-220] with a step size of 10. For each SNR, output parameters and their bias and CV were calculated. In the second simulation, SNR was fixed to 100, but f amounts varied between [0.03-0.30] with a step size of 0.01. Both simulations were done 10,000 times. Finally, a hybrid simulation was done to see which SNR was suitable for which f.

Another experiment was designed to study whether the threshold *b*-value was altering for different organs or not. The simulation was done with data given in Table 1, extracted from the literature.

II. Brain Data

The diffusion-weighted data set of a healthy

Table 1: Intravoxel incoherent motion (IVIM) parameters of organs

Organ	Diffusion coefficient (*D*)	Fraction of perfusion (*f*)	Pseudodiffusion coefficient (*D**)
Liver	0.0010	0.30	0.050
Kidney	0.0015	0.25	0.015
Brain	0.0010	0.05	0.010
Breast	0.0013	0.10	0.015

volunteer were acquired using a 3T Siemens MAGNETOM Prisma system; under a protocol approved by the Institutional Ethical Committee of Tehran University of Medical Sciences. The number of slices was 30. The echo time was set to 140 *msec* and the pulse repetition time to 8100 *msec*. The diffusion-weighted gradient settings used consisted of 11 *b*-values (b=0, 50, 100, 150, 200, 300, 400, 500, 600, 700, 800 s/mm^2). Five EPI/spin-echo (SE) diffusion-weighted pulse sequences were used with different acquisition matrices, resulting in different spatial resolutions. Acquisition matrices were 100×100, 128×128, 168×168, 198×198, and 242×242. All simulations and analyses have been done by MATLAB R2019b.

Results

Blood fraction effects on the accuracy of IVIM parameters were shown in Figure 1a. Coefficient variation (CV) (standard deviation of output parameter divided by its mean) and bias (the difference between the mean of estimated parameter and actual parameter) were used as two criteria for accuracy of outputs.

According to Figure 1a, CV and bias of perfusion parameters (f and D^*) decreased when blood fraction in voxel was large. On the other hand, bias and CV of D estimates increased when the blood fraction in a voxel was high. However, this increase was small enough that could be neglected. In this experiment, for a fixed SNR=100, f varied in the range of physiologic organs like the brain and liver (between 0.04-0.4).

In another simulation, the blood fraction was assumed to be fixed (f=0.1). The validity of IVIM parameters was calculated for several SNR (40, 50, 60, 70, 80, 90, 100, 110, 120, 130, 140, 150, 160, 170, 180, 190, 200, 210, 220). Figure 1b showed how SNR affected CV and bias of estimated parameters. The SNR affected the accuracy of parameters dramatically, as it could be predicted. The higher the imaging SNR setting, the higher accuracy, i.e.

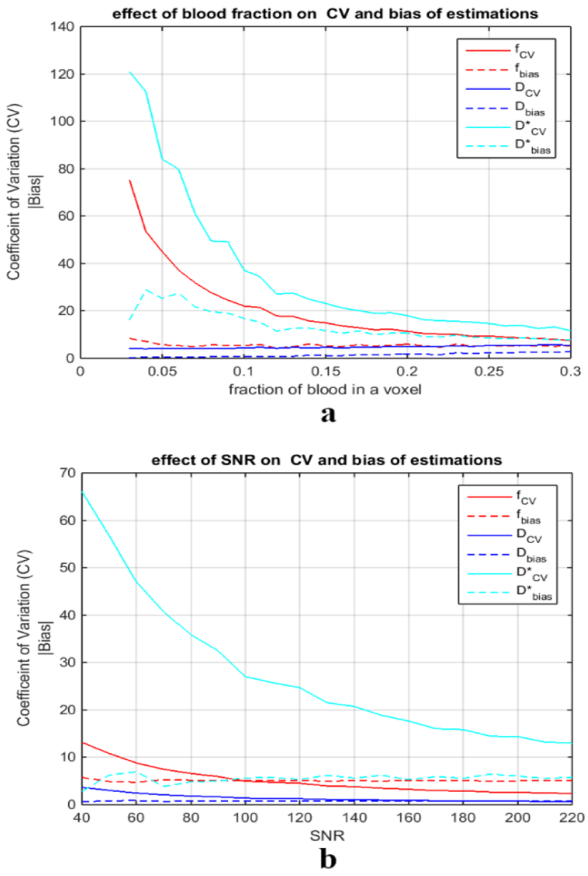

Figure 1: (**a**) Blood fraction effects on parameters validity, coefficient of variation (CV), and bias of Intravoxel incoherent motion (IVIM) parameters were illustrated for varying fraction of perfusion (f) [0.03 0.3] and fixed signal to noise ratio (SNR) = 100, (**b**) SNR effects on parameters validity, CV, and bias of output parameters were illustrated for varying SNR [40: 10: 220] and fixed blood fraction = 0.1

both CV and bias become less. Finally, the effects of both SNR and blood fraction on the validity of IVIM parameters were investigated and depicted in Figure 2. It demonstrated that CV and bias of f and especially D^* raised up when SNR and blood fraction were lower. However, the CV and bias changes of D were small.

Signal intensity, diffusion portion of signal intensity, and perfusion portion of signal intensity for brain, breast, liver, kidney, and noise floor are shown in Figure 3. Perfusion

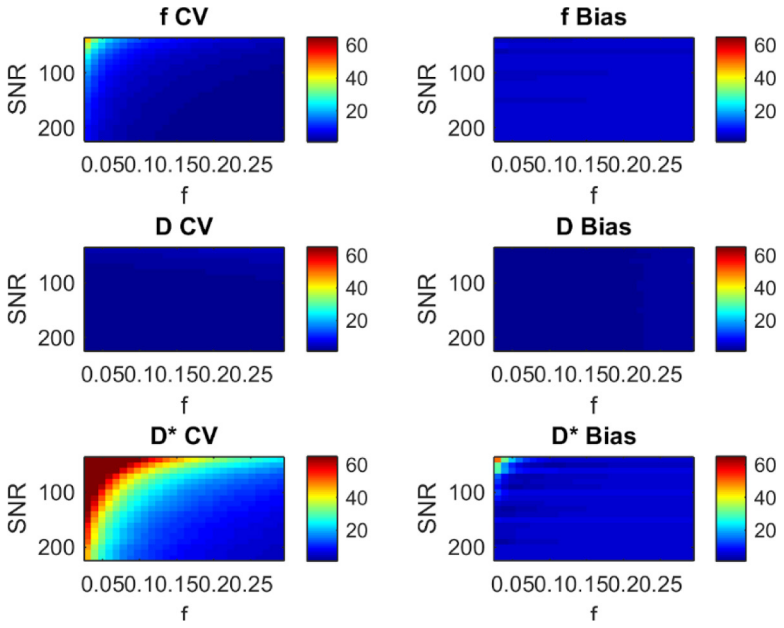

Figure 2: Coefficient of variation (CV) of parameters when both fraction of perfusion (*f*) and signal to noise ratio (SNR) were varying, changes in iffusion coefficient (*D*) were not significant, but variations in the validity of pseudodiffusion coefficient (D^*) were observable

signal intensities of high *b*-values were close to zero and even were smaller than the noise floor. Figure 3 showed that in a fixed SNR, capillary network pseudodiffusion and blood portion in each voxel affected perfusion signal decay and threshold *b*-value. However, the perfusion portion of the signal without motion-sensitizing gradient was just determined by *f*, speed of blood flow, linked to D^* helped perfusion signal decay occurred faster as well, and consequently, threshold *b*-value became lower.

Effect of matrix size on SNR has been shown in Figure 4 for the brain data with different matrices size (242×242, 198×198, 168×168, 128×128, and 100×100). The smaller the matrix size was chosen, the higher SNR was given. Figure 4 depicted how various matrix sizes resulted in changes in SNR.

Discussion

IVIM imaging is widely used today, and is also capable of extracting simultaneously functional and structural maps. IVIM model has 3 outputs: Diffusion (*D*), blood fraction (*f*) and pseudodiffusion (D^*). Estimates of *D* are more robust than those of *f* and D^*. Estimates of *f* and D^* are vulnerable to contamination by noise. Using the IVIM imaging in different organs with the same setting may lead to an inaccurate result.

Each organ has a specific amount of blood fraction in each voxel, determining how much intensity of the signal is perfusion portion when there is no motion-sensitizing gradient. *In-silico* simulation results showed that blood fraction affected the accuracy of parameters, especially *f* and D^* even if SNR is good enough. Results also indicated that the validity of perfusion parameters (*f* , D^*) increased when blood fraction was higher in a voxel. The more fraction of blood in each voxel, the more accurate *f* and D^*. For example, the blood fraction of kidney is about 25 percent of each voxel that is six to five times greater than the blood fraction of brain, which is about 4 percent. Therefore bias and CV of IVIM parameters in kidney are more acceptable in comparison with brain. This instinctive characteristic of each organ -blood fraction- can affect their IVIM-output parameters validity. To compensate for this issue, we should con-

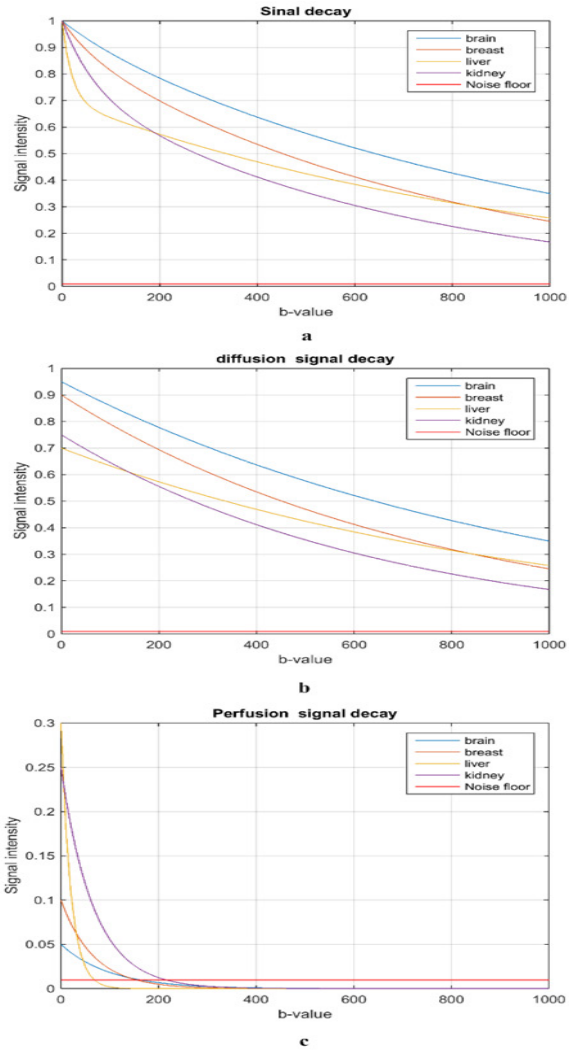

Figure 3: Perfusion portion of signal intensity plummet quickly by increasing *b*-value, optimum *b*-values was less than b where perfusion signal intensity reached noise floor. (**a**) Signal intensity (**b**) Diffusion portion of signal intensity and (**c**) Perfusion portion of signal intensity

trol imaging parameters to increase SNR and make the signal free of noise.

Our results confirmed that the higher SNR of images resulted in the more valid parameters, however, the high SNR expenses would be paid with less resolution. For instance, the resolution of brain IVIM imaging must be less than kidney IVIM imaging if the same validity is expected by the same hardware setting.

On this basis, before starting IVIM imaging, control parameters such as field of view (FOV), resolution matrix, and bandwidth (BW) should be calculated and updated for each specific organ. Since FOV is determined by organ dimensions and its location in the body, it is almost unchangeable for each organ. BW affects SNR, chemical shift, and acquisition time. Therefore, it is better to adjust the control parameters so that the signal output has an acceptable SNR in a reasonable acquisition time. Furthermore, chemical shift curbs the variation of BW. The main magnetic field is a hardware limitation and is not under our control. The only option, which is under control, is matrix size. A simple experiment was designed to investigate the impacts of SNR on IVIM imaging. A healthy brain was imaged in the same setting except for matrix resolution. It has been shown that matrix resolution affected SNR and subsequently the validity of IVIM parameters.

Resolution, magnetic field, acquisition time, and organ studied should be considered before the beginning of an IVIM imaging. To the best of our knowledge, because of the lack of validity of D^*, most IVIM studies in brain field have used just D and f in their analysis and D^* Using nonlinear methods such as neural networks and ICA is a new promising solution to overcome the lack of SNR [26].

Signal decay is because of water molecules displacements. Since blood displacements are greater than those of self-diffusion, then the perfusion signal vanishes in a high *b*-values regime. As a result, diffusion signal decay can be detected, and true D is calculable. Irrespective of D^*, blood fraction in each voxel is a critical factor. For example, D^* of kidney is larger than those of brain. However, its perfusion signal fades slower due to a bigger fraction of blood. As long as there are various amounts of f and D^* for each organ, the threshold *b*-value is especial for each organ. Our results suggest using *b*-values bigger than 300 s/mm^2 is crucial to obtain an insensitive diffusion coefficient using that is in compliance with Freiman finding [24].

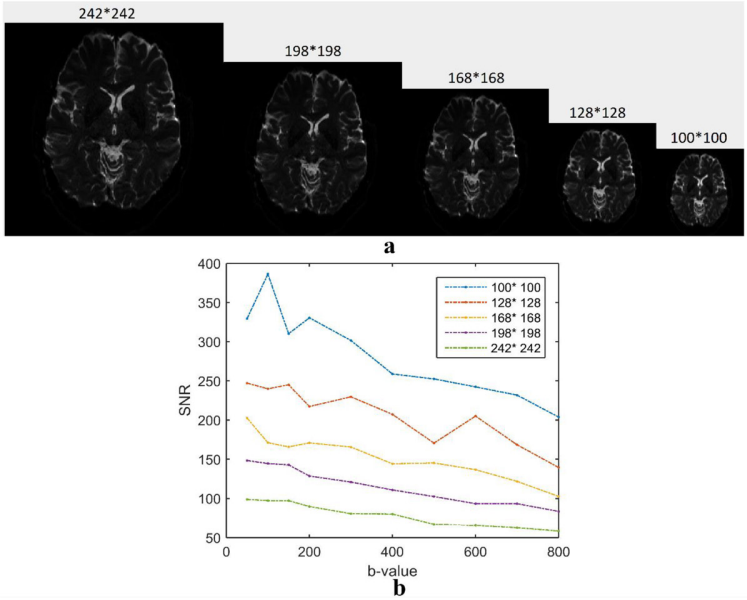

Figure 4: (**a**) 5 different resolutions of brain image with different matrices size, (**b**) decreasing signal to noise ratio (SNR) by increasing matrix size and also higher *b*-values were depicted, increasing fluctuation could be because of noise

Conclusion

IVIM model is a promising solution for finding both information of anatomical and physiological of organs simultaneously and non-invasively. IVIM imaging is a valuable MRI technique because it can get perfusion maps in addition to diffusion mas without using any contrast agents. However, the validity of its parameter should be considered carefully. The validity and accuracy of IVIM parameters are highly influenced by the SNR of imaging and the fraction of blood in the capillary network of each organ. This study suggests adjusting control parameters for distinct organs.

Acknowledgment

Authors gratefully acknowledge the use of MR imaging facilities of the National Brain Mapping Laboratory (NBML) in Tehran, Iran.

Authors' Contribution

All authors contributed to the study's conception and design. S. Sharifzadeh Javidi performed data collection and analysis. The first draft of the manuscript was written by S. Sharifzadeh Javidi. AR. Shirazinodeh and HR. Salighehrad commented on previous versions of the manuscript. All authors read and approved the final manuscript.

Ethical Approval

All experimental procedures were conducted according to The Declaration of Helsinki; written informed consent was obtained from participants, and the research was approved by the Institutional Ethical Committee of Tehran University of Medical Sciences (Approval code: IR.TUMS.MEDICINE.REC.1396.4257).

Funding

This project was supported by Tehran University of Medical Sciences Grant No. 9321345002 (36937).

Conflict of Interest

None

References

1. Stejskal EO, Tanner JE. Spin diffusion measurements: spin echoes in the presence of a time-dependent field gradient. *The Journal of Chemical Physics*. 1965;**42**(1):288-92. doi: 10.1063/1.1695690.
2. Le Bihan D, Breton E, Lallemand D, Grenier P, et al. MR imaging of intravoxel incoherent motions: application to diffusion and perfusion in neurologic disorders. *Radiology*. 1986;**161**(2):401-7. doi: 10.1148/radiology.161.2.3763909. PubMed PMID: 3763909.

3. Le Bihan D, Breton E, Lallemand D, Aubin ML, Vignaud J, Laval-Jeantet M. Separation of diffusion and perfusion in intravoxel incoherent motion MR imaging. *Radiology.* 1988;**168**(2):497-505. doi: 10.1148/radiology.168.2.3393671. PubMed PMID: 3393671.
4. Le Bihan D. What can we see with IVIM MRI? *Neuroimage.* 2019;**187**:56-67. doi: 10.1016/j.neuroimage.2017.12.062. PubMed PMID: 29277647.
5. Luciani A, Vignaud A, Cavet M, Tran Van Nhieu J, et al. Liver cirrhosis: intravoxel incoherent motion MR imaging—pilot study. *Radiology*. 2008;**249**(3):891-9. doi: 10.1148/radiol.2493080080. PubMed PMID: 19011186.
6. Federau C, Nguyen A, Christensen S, Saba L, Wintermark M. Cerebral perfusion measurement in brain death with intravoxel incoherent motion imaging. *Neurovascular Imaging.* 2016;**2**(1):1-5. doi: 10.1186/s40809-016-0020-7.
7. Ichikawa S, Motosugi U, Ichikawa T, Sano K, et al. Intravoxel incoherent motion imaging of the kidney: alterations in diffusion and perfusion in patients with renal dysfunction. *J Magn Reson Imaging.* 2013;**31**(3):414-7. doi: 10.1016/j.mri.2012.08.004. PubMed PMID: 23102943.
8. Sigmund EE, Cho GY, Kim S, Finn M, et al. Intravoxel incoherent motion imaging of tumor microenvironment in locally advanced breast cancer. *Magnetic Resonance in Medicine.* 2011;**65**(5):1437-47. doi: 10.1002/mrm.22740. PubMed PMID: 21287591. PubMed PMCID: 4692245.
9. Cheng ZY, Feng YZ, Hu JJ, et al. Intravoxel incoherent motion imaging of the kidney: The application in patients with hyperuricemia. *J Magn Reson Imaging.* 2020;**51**(3):833-40. doi: 10.1002/jmri.26861. PubMed PMID: 31318112.
10. Beyhan M, Sade R, Koc E, Adanur S, Kantarci M. The evaluation of prostate lesions with IVIM DWI and MR perfusion parameters at 3T MRI. *Radiol Med.* 2019;**124**(2):87-93. doi: 10.1007/s11547-018-0930-3. PubMed PMID: 30276599.
11. Bihan DL, Turner R. The capillary network: a link between IVIM and classical perfusion. *Magn Reson Med.* 1992;**27**(1):171-8. doi: 10.1002/mrm.1910270116. PubMed PMID: 1435202.
12. Lee EY, Hui ES, Chan KK, Tse KY, Kwong WK, Chang TY, Chan Q, Khong PL. Relationship between intravoxel incoherent motion diffusion-weighted MRI and dynamic contrast-enhanced MRI in tissue perfusion of cervical cancers. *J Magn Reson Imaging.* 2015;**42**(2):454-9. doi: 10.1002/jmri.24808. PubMed PMID: 25413245.
13. Federau C, O'Brien K, Meuli R, Hagmann P, Maeder P. Measuring brain perfusion with intravoxel incoherent motion (IVIM): initial clinical experience. *J Magn Reson Imaging.* 2014;**39**(3):624-32. doi: 10.1002/jmri.24195. PubMed PMID: 24068649.
14. Lin Y, Li J, Zhang Z, Xu Q, Zhou Z, et al. Comparison of intravoxel incoherent motion diffusion-weighted MR imaging and arterial spin labeling MR imaging in gliomas. *Biomed Res Int.* 2015;**2015**:234245. doi: 10.1155/2015/234245. PubMed PMID: 25945328. PubMed PMCID: 4402183.
15. Stieb S, Boss A, Wurnig MC, et al. Non-parametric intravoxel incoherent motion analysis in patients with intracranial lesions: test-retest reliability and correlation with arterial spin labeling. *Neuroimage Clin.* 2016;**11**:780-8. doi: 10.1016/j.nicl.2016.05.022. PubMed PMID: 27354956. PubMed PMCID: 4910187.
16. Le Bihan D. Diffusion, confusion and functional MRI. *Neuroimage.* 2012;**62**(2):1131-6. doi: 10.1016/j.neuroimage.2011.09.058. PubMed PMID: 21985905.
17. Cui Y, Dyvorne H, Besa C, Cooper N, Taouli B. IVIM Diffusion-weighted Imaging of the Liver at 3.0 T: Comparison with 1.5 T. *Eur J Radiol Open.* 2015;**2**:123-8. doi: 10.1016/j.ejro.2015.08.001. PubMed PMID: 26393236. PubMed PMCID: 4573456.
18. Barbieri S, Donati OF, Froehlich JM, Thoeny HC. Impact of the calculation algorithm on biexponential fitting of diffusion-weighted MRI in upper abdominal organs. *Magn Reson Med.* 2016;**75**(5):2175-84. doi: 10.1002/mrm.25765. PubMed PMID: 26059232.
19. Jalnefjord O, Andersson M, Montelius M, Starck G, et al. Comparison of methods for estimation of the intravoxel incoherent motion (IVIM) diffusion coefficient (D) and perfusion fraction (f). *MAGMA.* 2018;**31**(6):715-23. doi: 10.1007/s10334-018-0697-5. PubMed PMID: 30116979.
20. While PT. A comparative simulation study of bayesian fitting approaches to intravoxel incoherent motion modeling in diffusion-weighted MRI. *Magn Reson Med.* 2017;**78**(6):2373-87. doi: 10.1002/mrm.26598. PubMed PMID: 28370232.
21. Ye C, Xu D, Qin Y, Wang L, et al. Estimation of intravoxel incoherent motion parameters using low b-values. *PloS One.* 2019;**14**(2):e0211911. doi: 10.1371/journal.pone.0211911. PubMed PMID: 30726298. PubMed PMCID: 6364995.
22. Cho GY, Moy L, Zhang JL, et al. Comparison of fitting methods and b-value sampling strategies for intravoxel incoherent motion in breast cancer. *Magn Reson Med.* 2015;**74**(4):1077-85. doi: 10.1002/mrm.25484. PubMed PMID: 25302780. PubMed PMCID: 4439397.
23. Dyvorne H, Jajamovich G, Kakite S, Kuehn B, Taouli B. Intravoxel incoherent motion diffusion imaging of the liver: optimal b-value subsampling and impact on parameter precision and reproducibility. *Eur J Radiol.* 2014;**83**(12):2109-13. doi: 10.1016/j.ejrad.2014.09.003. PubMed PMID: 25277521. PubMed PMCID: 4254063.
24. Freiman M, Voss SD, Mulkern RV, et al. In vivo assessment of optimal b-value range for perfusion-insensitive apparent diffusion coefficient imaging. *Med Phys.* 2012;**39**(8):4832-9. doi: 10.1118/1.4736516. PubMed PMID: 22894409. PubMed PMCID: 3411587.
25. Lemke A, Stieltjes B, Schad LR, Laun FB. Toward an optimal distribution of b values for intravoxel incoherent motion imaging. *Magn Reson Imaging.* 2011;**29**(6):766-76. doi: 10.1016/j.mri.2011.03.004. PubMed PMID: 21549538.
26. Bertleff M, Domsch S, Weingärtner S, et al. Diffusion parameter mapping with the combined intravoxel incoherent motion and kurtosis model using artificial neural networks at 3 T. *NMR Biomed.* 2017;**30**(12):e3833. doi: 10.1002/nbm.3833. PubMed PMID: 28960549.